RICH DETECTOR FOR THE EIC'S FORWARD REGION PARTICLE IDENTIFICATION

An EIC R&D Proposal

December 13, 2013

Marco Contalbrigo[a], Marcel Demarteau[b], J. Matthew Durham[c], Hubert van Hecke[c](co-PI), Jin Huang[c], Ming Liu[c], Patrizia Rossi[d], Yi Qiang[d,*](co-PI, contact), Robert Wagner[b], Carl Zorn[d]

a. INFN, Sezione di Ferrara, 44100 Ferrara, Italy
b. Argonne National Lab, Argonne, IL 60439
c. Los Alamos National Lab, Los Alamos, NM 87545
d. Jefferson Lab, Newport News, VA 23606

* Email: yqiang@jlab.org

Table of Contents

RICH DETECTOR FOR THE EIC'S FORWARD REGION PARTICLE IDENTIFICATION

December 13, 2013

Abstract

An R&D program is proposed to investigate the technology used for a Ring Imaging Cherenkov (RICH) detector for the hadron particle identification in the forward region of the future Electron-Ion Collider (EIC). Both the dual-radiator RICH option and a modular RICH concept will be investigated and the associated special optics design will be carried out. In particular, a newly developed Large-Area Picoseconds Photo-Detector (LAPPD) using renovated Micro-Channel Plate (MCP) technology will be carefully evaluated as the readout of the RICH detector. If feasible, the excellent timing resolution provided by this new readout will greatly improve the PID capability of the RICH detector. A GEM-based readout option will be investigated as well. At the end, the project will be able to determine the best detector technology and provide a conceptual design of the RICH detector for the EIC.

1. Motivation

The future Electron-Ion Collider (EIC) [1] will target on several hot physics topics, such as the nucleon tomography and quark orbital momentum accessible through the study of the generalized parton distributions (GPDs) and the transverse-momentum dependent parton distribution functions (TMDs), the quark hadronization in the nuclear medium and the hadron spectroscopy. A dedicated EIC detector is currently under development and its conceptual schematic is shown in Figure 1. It is very clear that new detector technologies are crucial to help achieve the ultimate physics goal.

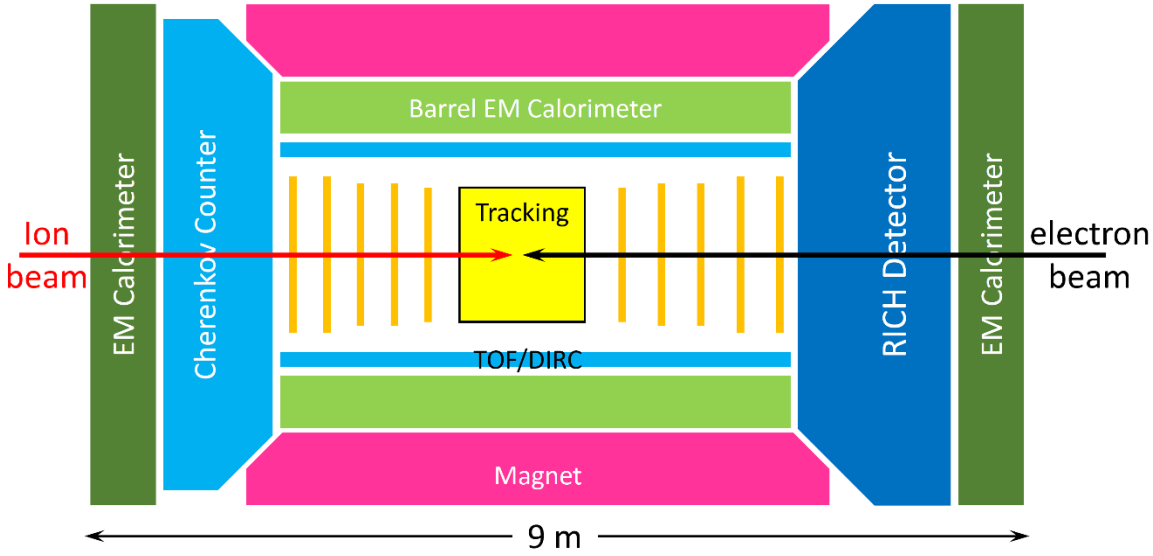

Figure 1 A schematic view of an EIC detector package.

In this proposal, we are mainly concerned with hadron identification in the forward and backward region (|*rapidity*| > 1). Using the semi-inclusive DIS (SIDIS) as an example, SIDIS is a powerful tool for disentangling the distributions for different quark and anti-quark flavors. It is also the golden channel to study the TMDs and further allow us to investigate the full three-dimensional dynamics of the nucleon. While detection of pions provides information mainly regarding light quarks, kaon identification is particularly important to study sea quark distributions. As shown in Figure 2, the momentum of SIDIS pions in the forward and backward region typically ranges from less than 1 GeV to about 15 GeV, and from Figure 3 we can see that pions greatly outnumber kaons over the whole kinematic region. In most of the momentum range the kaon yield is only about 10 – 15% of the pion yield. Therefore a 4σ K/π separation is desirable for clean kaon identification.

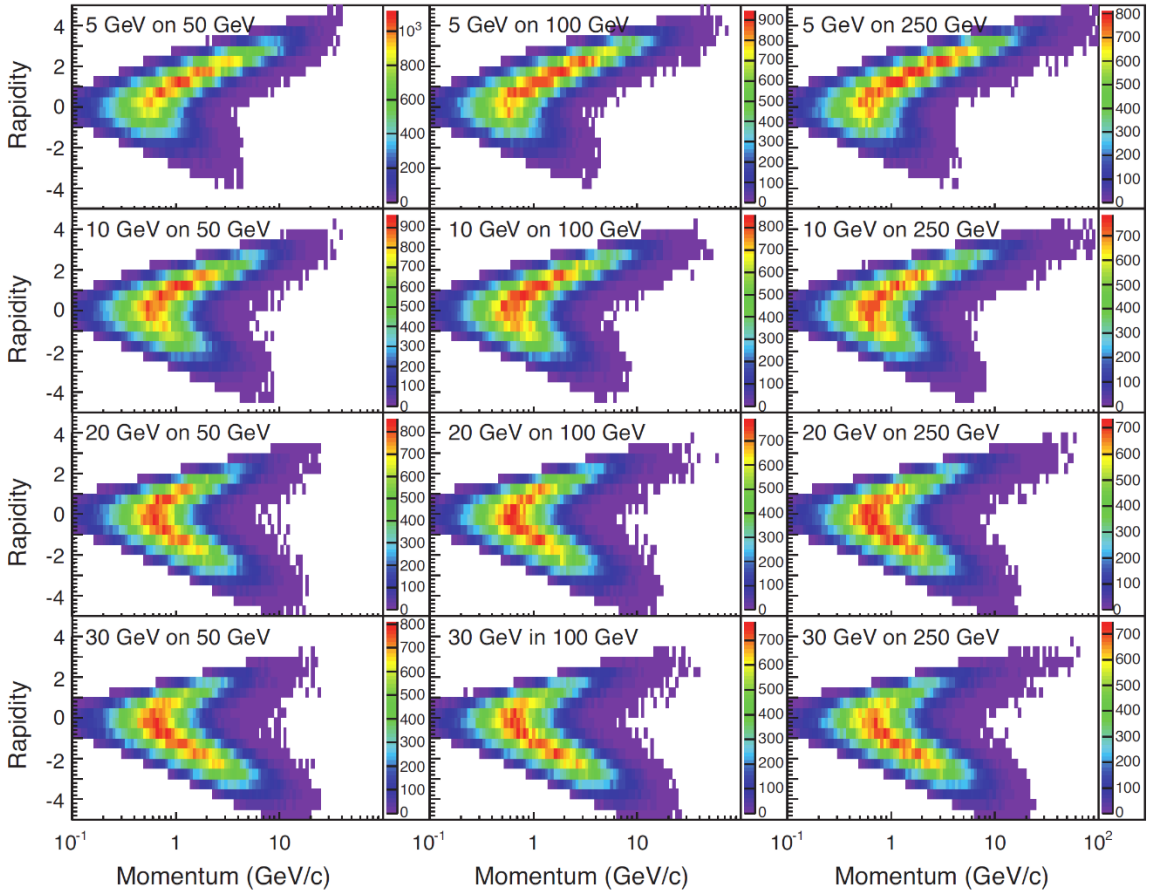

Figure 2 Momentum vs. rapidity in the laboratory frame for pions from semi-inclusive deep inelastic scattering (SIDIS) reactions [1]. The following cuts have been applied: $Q^2 > 1$ GeV^2, $0.01 < y < 0.95$ and $z > 0.1$.

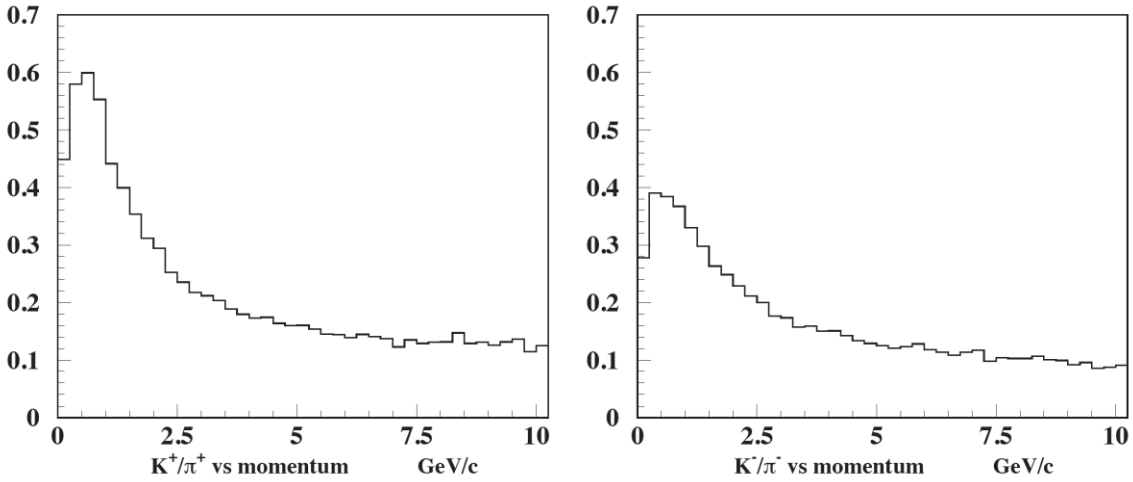

Figure 3 Kaon/pion ratio vs. momentum in the laboratory system from SIDIS events in the forward region (*rapidity* > 1 and for a 10×100 GeV configuration).

In order to cover such a large momentum range a combination of various particle identification technologies is needed. The low momentum range (0 – 5 GeV) can be covered by high resolution time-of-flight (TOF). Meanwhile, for the higher momentum range (5 – 15 GeV), the most viable detector options are Ring Imaging Cherenkov (RICH) detectors with dual radiators, or two RICH detectors with radiators of different refractive indices. Each radiator will provide unique sensitivities to different kinematic regions. As illustrated in Figure 4, an aerogel RICH detector would provide kaon identification for the intermediate x and Q^2 region, and a gas radiator would provide unique coverage in the high x and Q^2 region. In next section, we will discuss more details about the choice of different radiators and readout options.

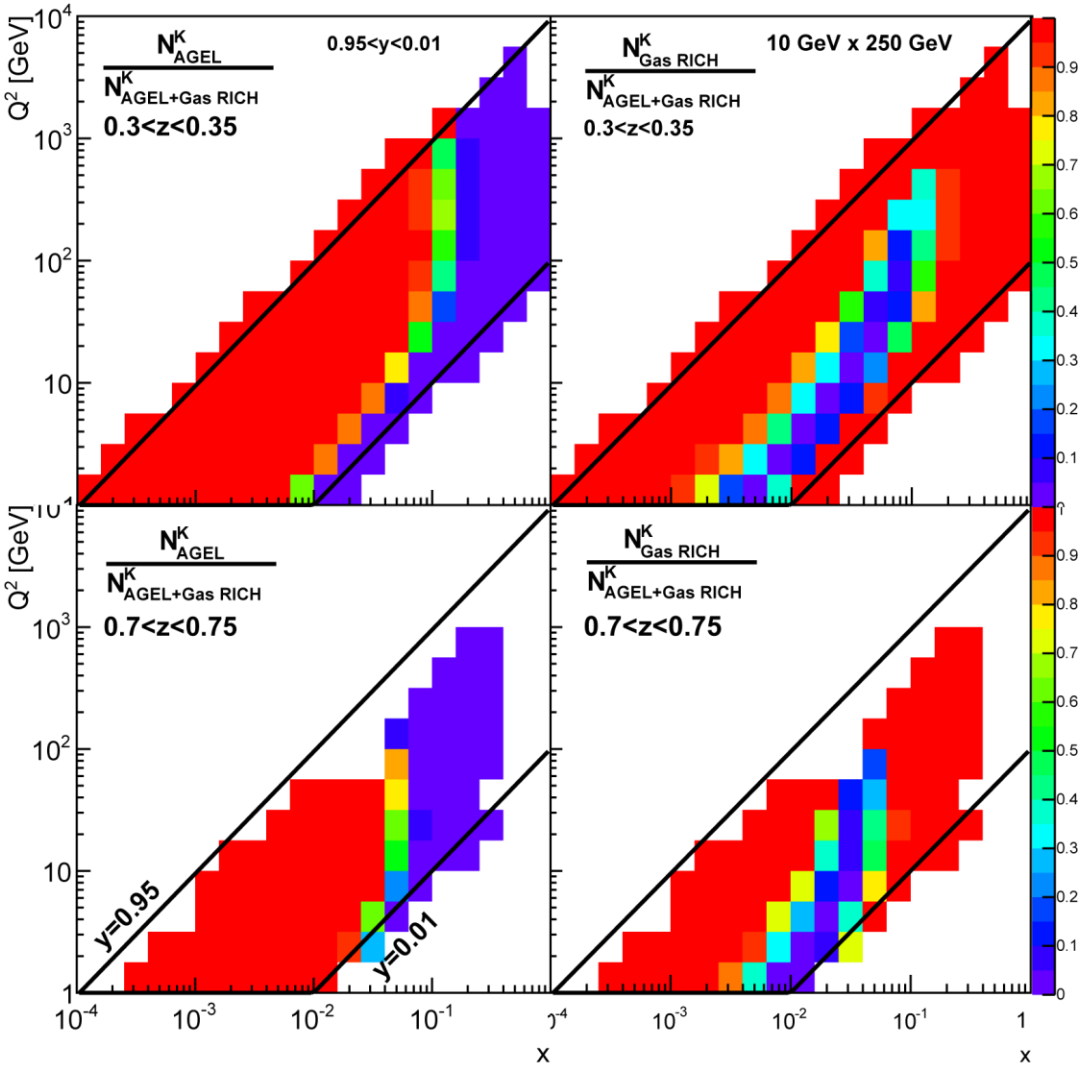

Figure 4. Yield ratios for SIDIS events with identified Kaons as function of x and Q^2, for an EIC detector with a barrel PID detector, a forward gas RICH and a forward aerogel RICH. Shown are the ratios when the forward gas RICH (left) or the forward aerogel RICH (right) are removed. Higher and lower z-ranges are shown in the top and bottom rows. This particular study is from the ePHENIX letter of intent [2], for a 10×250 GeV beam configuration.

2. Technology Overview

2.1. Choice of Radiators

Table 1 List of properties of commonly used Cherenkov radiators.

Material	Index	N_0 (cm^{-1})	Max Angle (rad)	Threshold (GeV)		
				Pion	K	Proton
N_2	1.000298	0.06	0.024	5.53	20.27	40.26
CO_2	1.000449	0.09	0.030	4.5	16.52	32.8
CF_4	1.000482	0.1	0.031	4.35	15.94	31.66
Freon 12 (CCl_2F_2)	1.001073	0.21	0.046	2.91	10.68	21.21
C_4F_{10}	1.00137	0.27	0.052	2.58	9.45	18.77
Aerogel 1.01	1.01	1.18	0.141	0.95	3.49	6.93
Aerogel 1.02	1.02	2.33	0.198	0.67	2.46	4.89
Aerogel 1.05	1.05	5.58	0.310	0.42	1.55	3.07
Freon (C_6F_{14})	1.2989	40.73	0.692	0.16	0.6	1.19
Fused Silica (SiO_2)	1.473	53.91	0.825	0.12	0.46	0.91

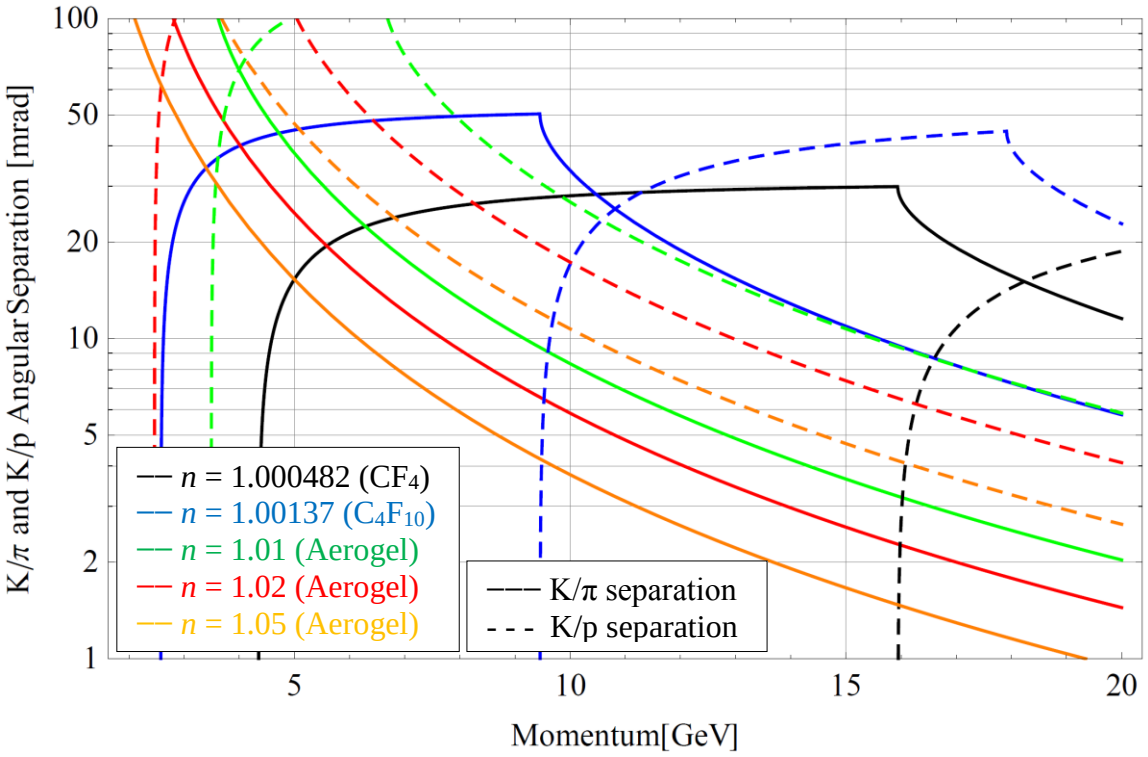

Figure 5 Angular difference of Cherenkov radiation produced by different charged particles.

As shown in Table 1 and Figure 5, in order to cover the mid-momentum range (5 – 10 GeV), the refractive index of the radiator needs to be between 1.01 and 1.05. In this range, silica aerogel is the only existing material. Silica aerogel has been used for decades in threshold Cherenkov counters for high energy physics, but more recently it has also been used as radiator material for RICH detectors in several particle physics experiments such as HERMES, LHCb, AMS, BELLE, etc. (See [3][4][5] and references therein). The optical properties of aerogel are crucial parameters for the performances of RICH detectors. For instance, any angular dispersion of the emitted photons affects the precision of the Cherenkov angle measurements. In addition, a high transparency (Transmittance) and a proper refractive index (n) are required in order to collect a sufficient number of photons for a reliable ring reconstruction. The measured transmittance T of an aerogel sample of thickness t, as function of the light wavelength λ is usually parameterized through the Hunt formula

$$T = Ae^{-Ct/\lambda^4}$$

which assumes that the absorption of the light, parameterized by A, is independent of the wavelength λ and that the Rayleigh scattering has a λ^{-4} dependence. The clarity coefficient C is proportional to the radiation scattered per unit of sample length, and is usually measured in $\mu m^4/cm$. Clarity is a measure of the quality of the sample - as C decreases more photons exit unscattered. Aerogel with a good optical quality therefore has values for A and C close to 1 and 0, respectively.

Absorption length (Λ_{abs}) and scattering length (Λ_{sc}) (in cm) are related to A and C through

$$\Lambda_{abs} = -t/\ln(A) \qquad \Lambda_{sc} = \lambda^4/C.$$

At present, aerogel tiles of large size and with good optical properties are produced by two Russian groups in Novosibirsk [6]. Samples of different refractive indices (n = 1.03, 1.04, 1.05), thicknesses and sizes, produced in different periods, have been characterized by the INFN group by means of a spectrophotometer and tested in dedicated test beams (CERN, INFN-LNF). The INFN group is currently building a proximity focusing RICH for the CLAS12 [7] spectrometer of Hall B at Jefferson Lab. The group also tested several aerogel samples produced in Japan by Matsushita-Panasonic [8] and by the US Aspen company [9], and is in contact with the Japanese group developing high-quality aerogel for the BELLE-II experiment [10].

In Figure 6 a comparison of the transmittance measured as a function of wavelength is presented for a 1 cm Matsushita tile (red) and a 2 cm and 3 cm Novosibirsk tiles (black and blue) for nominal refractive index n = 1.05. As can be seen, the Russian group is able to produce tiles of 2 cm thickness with the same transmittance as the 1 cm thickness (the only size available) produced by the Japanese company. At 400 nm, the measured transmittance for the Russian aerogel samples of 2 cm is of the order of ~ 65%. From these measurements the very good value of clarity of ~ 0.0050 $\mu m^4/cm$ for a refractive index of n = 1.05 has been extracted. In Figure 7 the transmittance of the n = 1.01 (blue)

and n = 1.05 (green, red and yellow) Aspen tiles compared with an n = 1.05 Novosibirsk tile (black) is shown. The better optical quality of the Russian aerogel is clearly evident.

The production of aerogel from the Russian groups was also monitored by the INFN group over a period of approximately one year, leading to a dramatic increase in the material's scattering length, as can be seen in Figure 8. The new generation aerogel from Novosibirsk demonstrated good performance, but further improvements in particular towards larger thickness and tile size could be necessary for the EIC RICH. Thus an R&D phase with the aerogel production company has to be foreseen for this project.

For the high-momentum range (10 – 15 GeV), a gas radiator needs to be considered. Due to the low yield of Cherenkov light in gas, a large volume of gas is needed to produce enough photons.

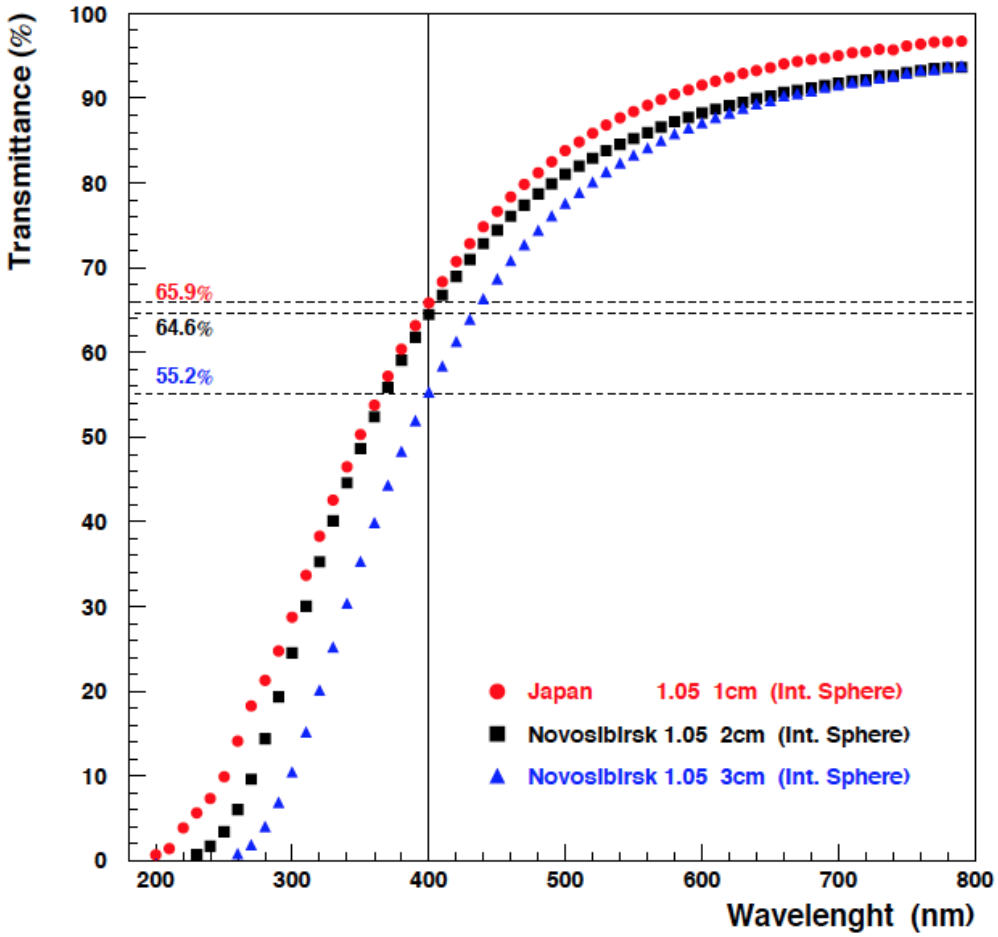

Figure 6 Comparison of the transmittance measured as a function of the wavelength for a 1 cm Matsushita tile (red) and a 2 cm and 3 cm Novosibirsk tiles (black and blue). All tiles have nominal refractive index n = 1.05.

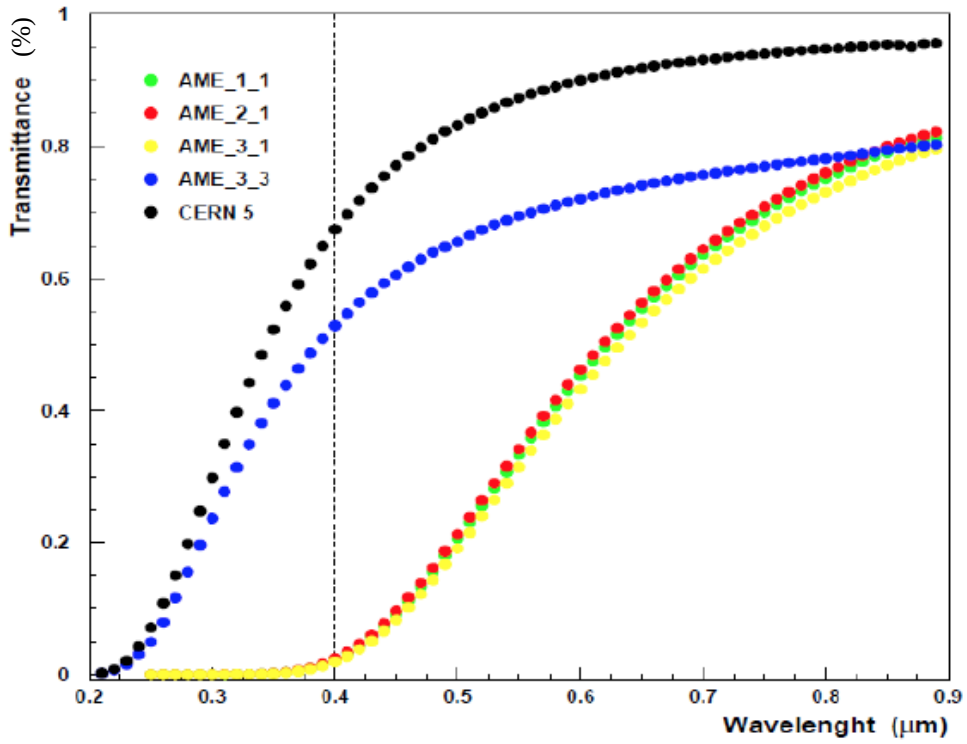

Figure 7 Transmittance of the n = 1.01 (blue) and n = 1.05 (green, red and yellow) 2 cm Aspen tiles compared with an n = 1.05 Novosibirsk tile (black).

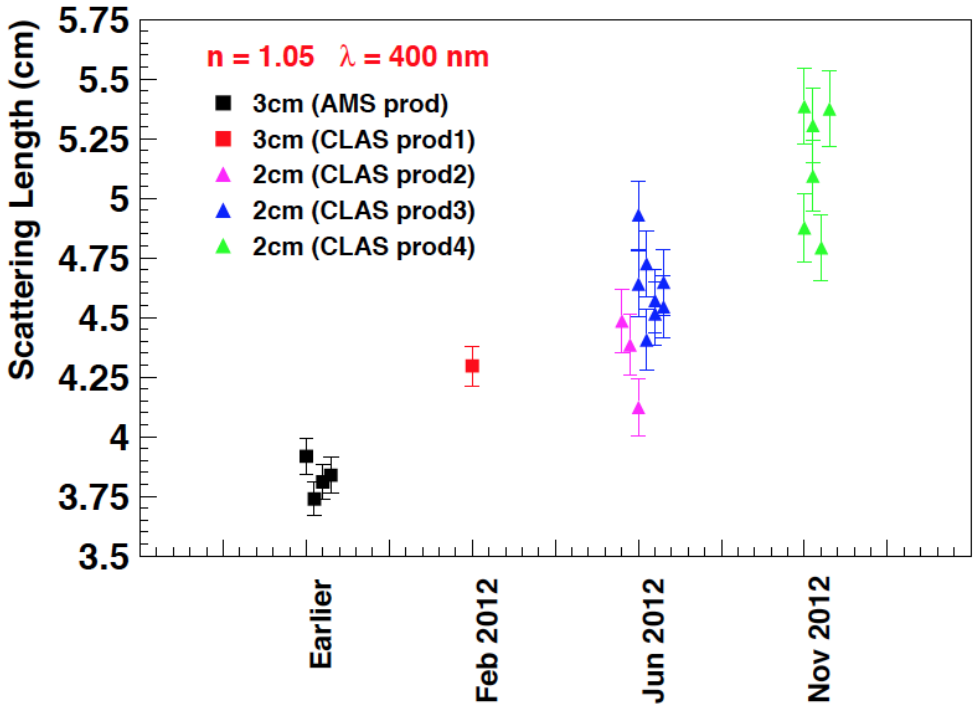

Figure 8. Scattering length at λ = 400 nm for n = 1.05 Novosibirsk tiles versus the production date.

2.2. Dual-Radiator Concept

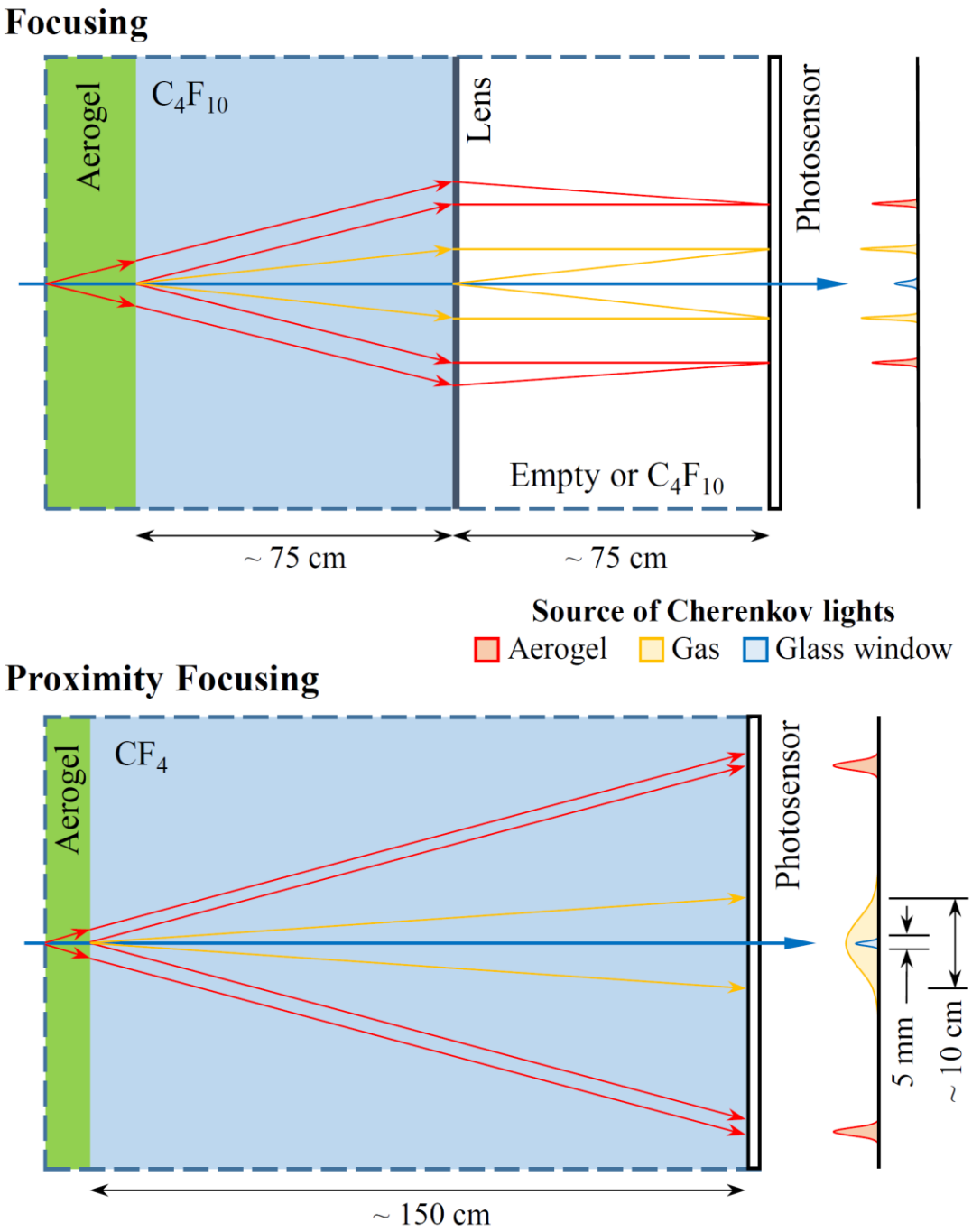

Figure 9. Concepts of dual-radiator RICH detector for the EIC. Top: a concept with focusing using a Fresnel lens; Bottom: a concept using proximity focusing.

A dual-radiator RICH detector has the advantage of a more compact size and lower cost by using a shared readout, when compared with two separate Cherenkov detectors. Figure 9 shows two concepts of dual-radiator RICH detectors for the EIC. The length of both devices is chosen to be about 150 cm, given the space available in the MEIC design.

The first concept shown on top is a focusing RICH detector. In this concept, an aerogel radiator is put in the front to cover the 5 – 10 GeV momentum range. Following the aerogel is a 75 cm long gas radiator volume containing C_4F_{10} to cover the 10 – 15 GeV range. The Cherenkov photons generated in each of the radiators are then focused by a Fresnel lens with a focal length of 75 cm. A super ultraviolet transmitting (SUVT) acrylic lens may be used to allow transmission of Cherenkov photons with wavelengths longer than 280 nm, as shown in Figure 10. With about 10 – 20 photoelectrons per Cherenkov ring, the required position resolution of the readout is a few millimeters in order to reach 4σ kaon/pion separation. Furthermore, because of the spatial resolution of the readout device, the photosensors don't need to be placed at the focal plane of the lens, but can be moved closer to reduce the total length of the detector.

The second concept is a proximity focusing RICH detector. The first radiator is still aerogel. In order to achieve a reasonable angular reconstruction with proximity focusing, the thickness of the aerogel has to be limited to a few centimeters and the readout needs to be far away. Hence a 150-cm long volume is left between aerogel and readout. This volume will be filled with CF_4 gas and serves as a threshold Cherenkov detector to veto pions up to 17 GeV. In the high momentum range (10 – 15 GeV), the separation of kaons and protons will still rely on aerogel. Although the proximity design seems much simpler in terms of optics design and mechanical construction, one big challenge will come from the Cherenkov radiation in the glass window of the readout sensors. Because of the photocathode coating, Cherenkov photons will exit the window and produce photoelectrons in the photocathode, instead of being trapped inside the window due to internal reflection. The hits generated by these photoelectrons will be concentric with the Cherenkov hits originated from CF_4. The coverage and amplitude of such a background signal depend on the window thickness. A 2 mm window typically generates about 10 photoelectrons with a spread of 5 mm. With a 2-dimensional readout, these signals from glass window can be removed by applying geometric cuts. Nevertheless, thinner windows will clearly help suppress this kind of background.

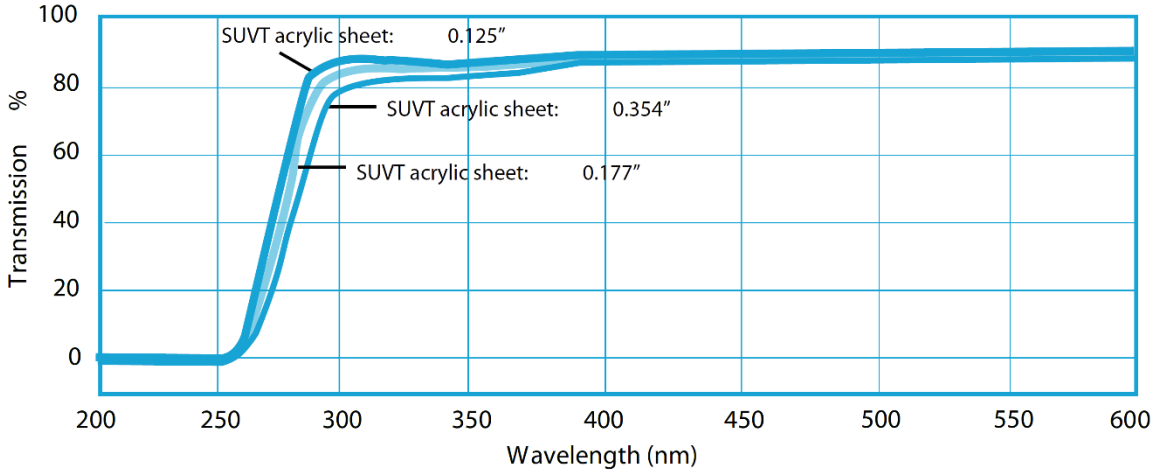

Figure 10 Transmission of super ultraviolet transmitting (SUVT) acrylic sheet [11].

Both concepts shown here are still in a very preliminary stage. More effort will definitely be needed to identify the best option with optimal optical design and an appropriate combination of radiators. These efforts are part of this proposed project.

2.3. Modular Concept

In parallel to the dual-radiator concept, we are developing a modular concept for aerogel RICH detectors. In this concept, we assume a separate gas RICH detector would provide high momentum hadron ID (e.g. the gas-RICH under the support of current proposal RD-6 [12]). Meanwhile, we will focus on the hadron PID between p = 1 – 10 GeV region using a single aerogel radiator.

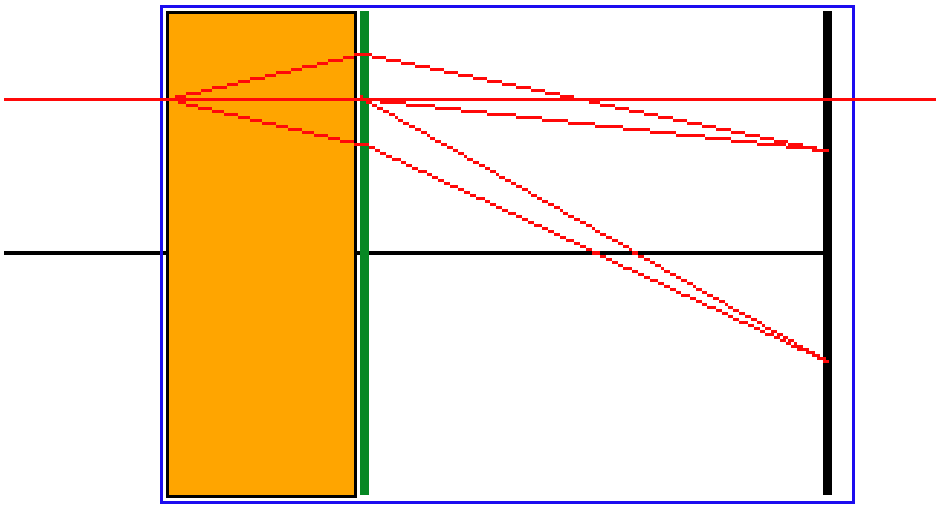

Figure 11. Diagram of a modular imaging aerogel detector, which consists of an aerogel radiator (orange), a Fresnel lens (green) and a photon detector (black). A module would be 10-20cm across.

In this scheme, a large detector would be built up out of small, independent units. A schematic of one unit is shown in Figure 11. Each unit would contain a Cherenkov radiator, in this case aerogel (orange), followed by an acrylic Fresnel lens (green), which focuses the Cherenkov photons onto a photon detector (black). In addition, the acrylic lens functions as a filter blocking scattered, low-wavelength photons. The scale of this unit would be determined by the size of the aerogel tiles used (assuming a single tile per unit), or by the size limitations of available Fresnel lenses or readout systems, but is expected to be of scale 10-20 cm. For particles that are incident parallel to the axis of the unit, Cherenkov rings would be centered in the unit's axis. The lens' focal length should be chosen such that the ring is smaller than the unit's diameter. Off-axis incident tracks result in rings offset from the center, but if the off-axis angular distribution is limited, the diameter of the sensitive area could be smaller than the size of the unit. The spatial resolution of the photon detector will be determined by the requirement that kaons and pions be distinguished at the upper end of the momentum range. Since the ring size in the

modular design is expected to be of order ~ 10 cm, the pixel size will likely be small, one-to-few mm.

Full simulation of these units in the experimental environment will determine the parameters of this scheme, such as the necessary resolution of the photon detector, the focal length *etc*. When more than one charged particle traverses a given module, position and momentum information available from other detectors will be used in combination with the ring-hit distributions to determine the particle identities. Detailed algorithms will be developed based on full simulations.

2.4. LAPPD Readout

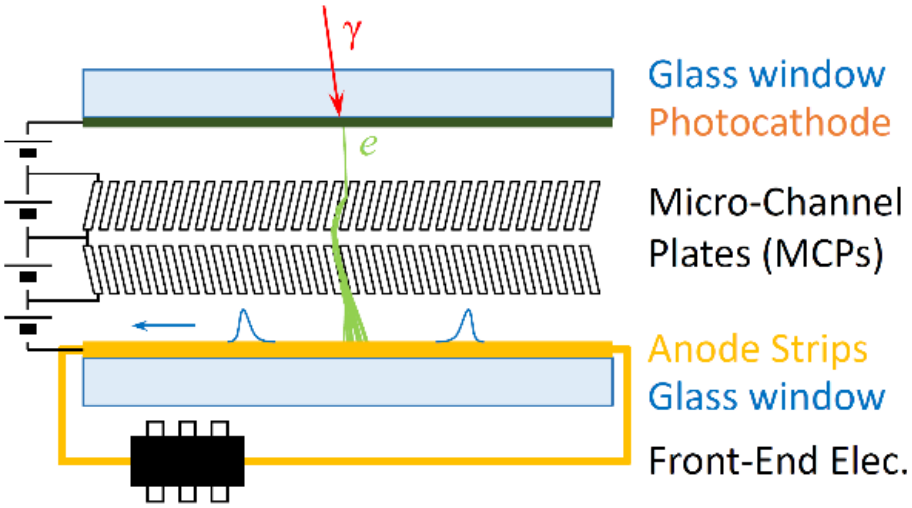

Figure 12 Schematic of the MCP-based LAPPD.

Starting in 2009, the development of a large-area picosecond-scale time resolution photo-detector has been carried out by the large-area picoseconds photo-detector (LAPPD) collaboration [13]. The goal of the R&D program is to develop a family of large-area robust photo-detectors that can be tailored for a wide variety of applications where large-area economical photon detection is needed. The approach is to apply micro-channel plate (MCP) technology to produce large-area photo-detectors with excellent space and time resolution. In addition to having excellent resolution, the new devices should be relatively economical to produce in quantity. Hence such a detector can be used in many applications, such as precision time-of-flight measurements, positron-emission tomography (PET) for medical imaging. Particularly, it provides a very attractive, low cost, high performance readout solution for imaging Cherenkov detectors.

Figure 12 shows a schematic of the MCP-based LAPPD detector [14]. Light is incident on a photocathode coated on the inner surface of the entrance window, producing electrons via the photoelectric effect. These electrons accelerate across a potential gap toward a pair of high-gain structures consisting of thin plates with high

secondary electron emission (SEE) enhanced, micro-engineered pores. Voltages of roughly 1 kV are applied across each plate. Each electron entering a pore accelerates and strikes the pore walls, producing an avalanche of secondary electrons. The avalanche builds until the amplified pulse exits the bottom of the second MCP. This electrical signal is collected on an anode structure at the bottom, and passes through the vacuum assembly to front-end electronics, which digitize the signal.

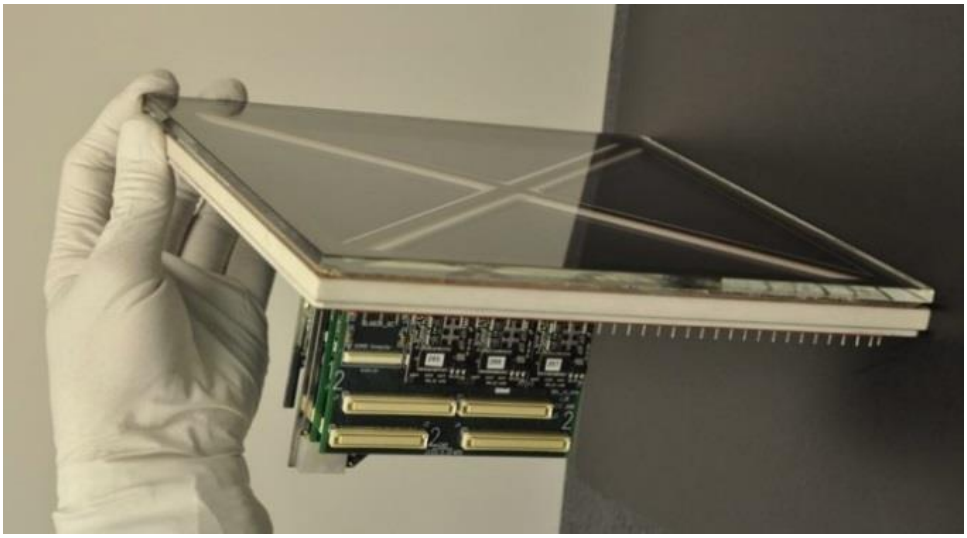

Figure 13 A 20×20 cm^2 LAPPD prototype with a ceramic body.

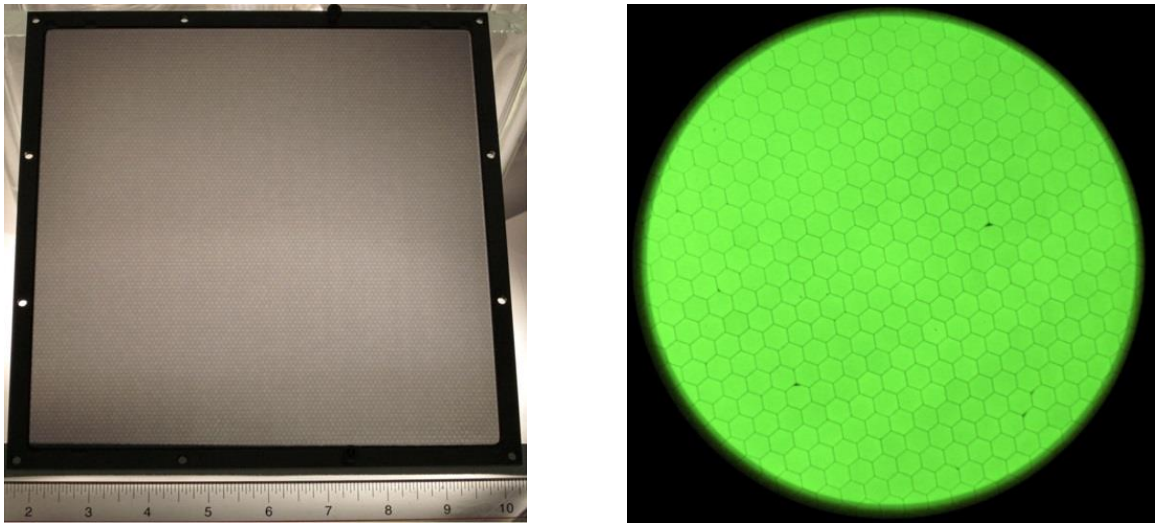

Figure 14 Left: photograph of a 20×20 cm^2 MCP made using ALD treatment of a borosilicate glass micro-capillary array. 20 μm pores, 1.2 mm thickness; Right: image for UV illumination onto an ALD coated borosilicate MCP with 20 μm pores, 1.2 mm thickness. The hexagonal multi-fiber packing structure is clearly visible.

The project is in its fourth year and excellent progress has been made. In particular, thermal evaporation has been used to form a photocathode on a large area glass window,

with quantum efficiency (QE) over 25% at 350 nm wavelength. The collaboration applied atomic layer deposition (ALD) on capillary glass channel substrates to produce MCPs [15] as shown in Figure 14, and has achieved better gain uniformity, longer life-time and more robust performance at much lower cost than standard commercial MCPs. The anode readout will use strip transmission lines [16] sampled by front-end waveform sampling chips [17]. The position of a hit along individual strips will be calculated based on the time difference of the signals reaching the two ends. The LAPPD collaboration has successfully assembled a ceramic body prototype with QE > 25% that successfully produced signals when excited with a UV laser inside the vacuum processing tank. The collaboration has also assembled a more economical all-glass detector package using an O-ring top window seal and an aluminum photocathode. This version has been operated for the past one and half years and has demonstrated single photoelectron time resolution of 44 ps. Small form factor samples with 6×6 cm^2 active area MCPs are expected to be fabricated in a vacuum transfer system at Argonne and should be available to early adopters in 2014.

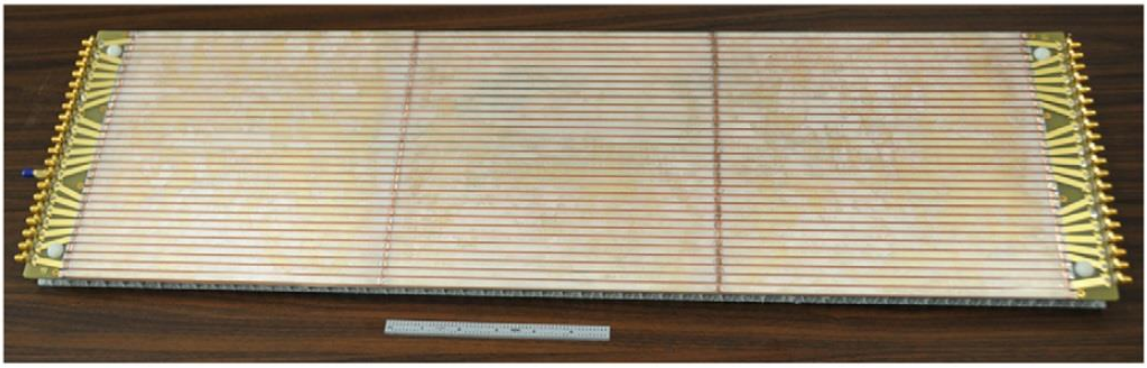

Figure 15 The 3-tile anode. The connections between anode strips on neighboring tiles have been made by soldering small strips of copper to the silver silk-screened strips on the glass [16].

When produced in large quantities, the manufacturing cost of LAPPDs is expected to be much cheaper than existing pixelated photo detectors, such as Silicon Photomultiplier (SiPM) and Multi-anode Photomultiplier Tubes (MaPMT), while still being able to provide comparable spatial resolution (~ 1 mm). The LAPPD uses a stripe-line readout anode which significantly reduces the total channel count, particularly for applications that need to cover a very large area such as a RICH detector. Under low rate conditions, the readout of tiles can be chained as shown in Figure 15 to further reduce the number of channels.

Another huge advantage that LAPPDs can bring is their exceptional time resolution. The uncertainty of the signal transition time in anode strips is only 17 ps [18] which provides a good determination of longitudinal position, as shown in Figure 16. The observed absolute timing resolution for single photon hits has been measured to be about 44 ps from a demountable LAPPD prototype using a metal photocathode. Therefore just by measuring the time of Cherenkov light hits, the LAPPD readout can be used as a very good time-of-flight detector for low momentum particle identification. Assuming that on

average 10 photon electrons are collected (from Cherenkov photons generated in 2 mm window glass), then the time resolution is expected to be better than 15 ps when convoluted with a beam's typical RF signal uncertainty. By looking at Figure 17, with a detection plane 4 meters away from the interaction point, the LAPPD can provide a 4σ kaon/pion separation up to 5 GeV.

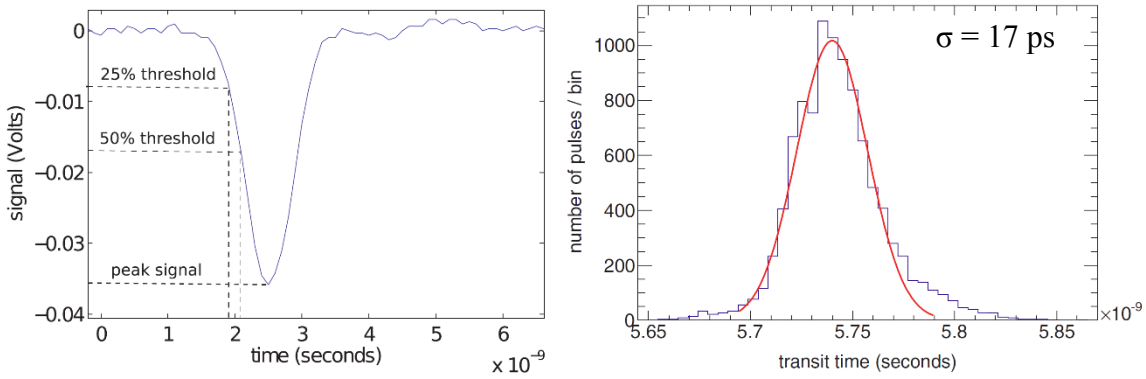

Figure 16 Left: an example of a MCP pulse showing the peak signal and the crossing time for a 50% and 25% constant fraction threshold. Right: measured time distribution of signals from a demountable LAPPD assembly using a focused 100-fs pulsed laser source [18].

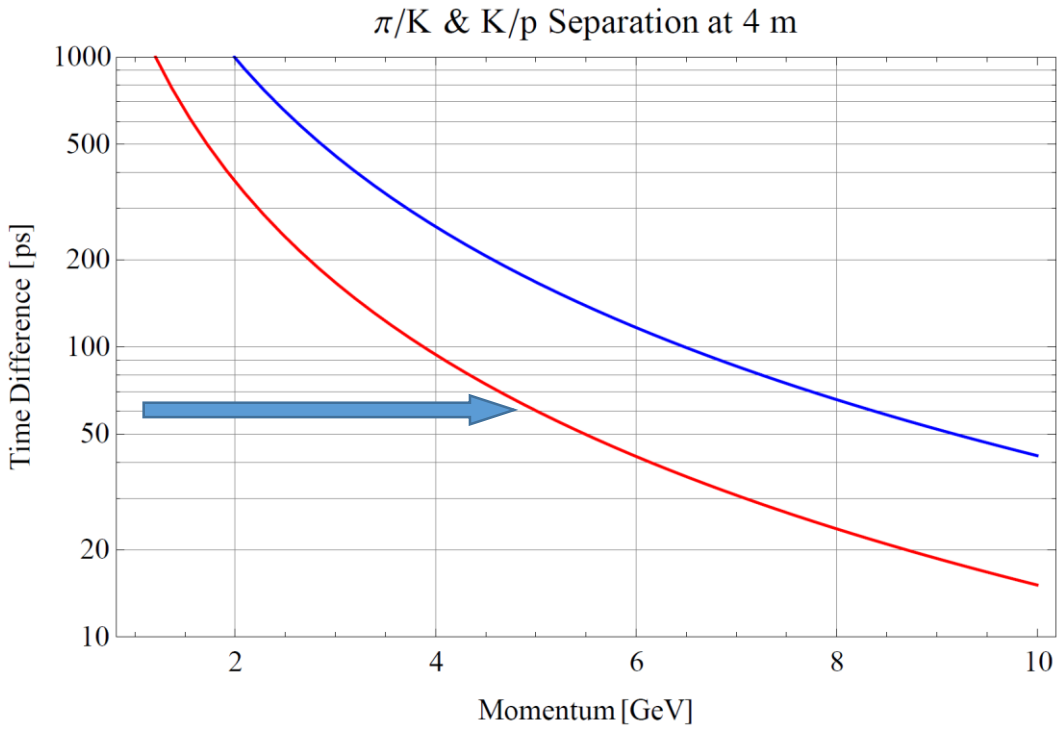

Figure 17 Difference in time-of-flight of kaon and pion and a path of 4 meters.

2.5. GEM-Based Readout

GEMs with a reflective photocathode film deposited on the uppermost surface have recently emerged as an attractive photon detection technology [19], see Figure 18. Since the amplification structure is effectively decoupled from the charge collection plane, the geometry of the readout pattern can be optimized for the desired resolution with a minimal channel count. GEMs are available in various sizes from a range of foreign and domestic manufacturers. GEMs function well in magnetic fields. They have also been shown to operate in a variety of gases that are transparent in the wavelength range of interest, which minimizes Cherenkov photon losses.

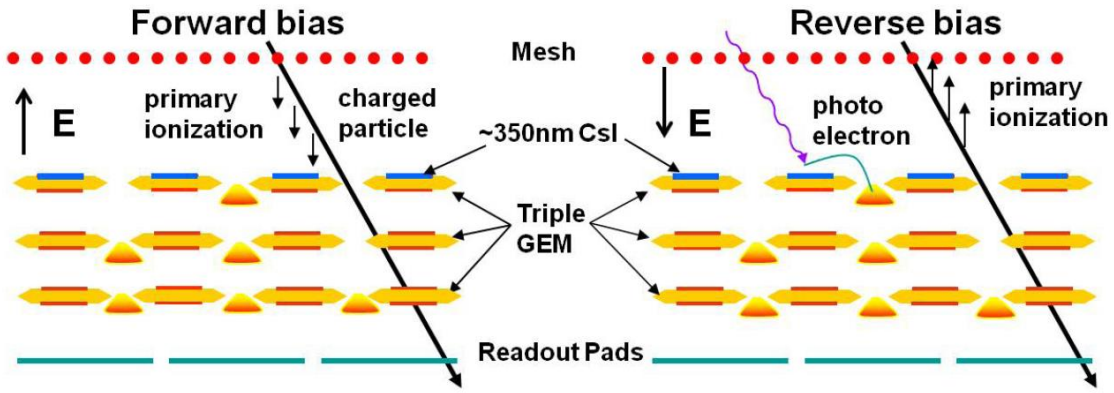

Figure 18 Triple GEM stack operated in the standard forward bias mode (left) and in the hadron-blind reverse bias mode (right) [19].

In the wavelength range of interest for unscattered Cherenkov photons produced in aerogel, ~ 300 – 500 nm, bialkali crystals such as Sb-Cs-K have the necessary quantum efficiency (QE) to function as photocathodes as shown in Figure 19. Early studies by Breskin *et al.* [20] have shown a reasonable QE when deposited onto GEM foils. However, the effective QE is also strongly dependent on the choice of gas, which affects photoelectron scattering back into the photocathode.

Part of this research will therefore be to find the appropriate gas or mixture of gases to maximize the collected photoelectron yield in the visible range. Bialkali photocathodes are notoriously reactive with oxygen, and therefore the detector must be assembled without exposure to oxygen. However, the relatively small size and modular nature of the design considerably simplifies this task. In addition, the design of the detector greatly simplifies maintenance during operation and allows for straightforward replacement of individual modules, if necessary.

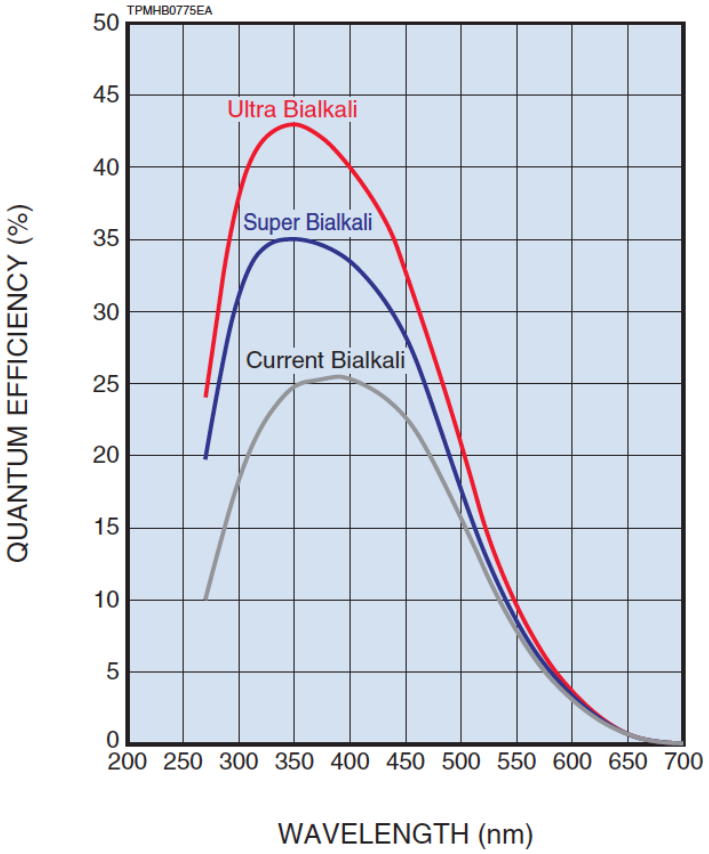

Figure 19 Typical quantum efficiency curves for bialkali photocathodes from Hamamatsu Photonics Corporation.

3. Goals and R&D Activities

The goal of the project is to determine the detector technology and finish the conceptual design of the RICH detector in a course of three years.

We will carry out feasibility studies in various aspects toward a conceptual design. We plan to perform detector simulations to optimize the detector parameters and provide requirements on different components. We will also investigate the feasibly of several novel readout options, including the newly developed budget-friendly MCP-based LAPPD photodetectors and the GEM-based readout. R&D on the LAPPD will be conducted as well so that such readout can better fit EIC's requirements. Meanwhile we will proceed with the characterization and selection of aerogel radiators.

Upon the completion of the project, with the chosen detector technology and the conceptual design, further work is anticipated producing prototypes of such RICH detectors for the EIC.

3.1. Detector Simulation and Conceptual Design

The detector simulations will be carried at Jefferson Lab and LANL. We will take advantage of existing EIC simulation codes developed by other EIC projects, and focus on simulation of detector performance, optimization and optics design.

Many of the parameters of the design need to be studied with detailed simulations: modeling of the aerogel, including realistic values for clarity, absorption length, refractive index non-uniformity and dependence on wavelength, coupled with the optical properties of the lens and the photon detector will determine the number of photons detected per ring. These studies will also show the wavelength distribution of photons in the Cherenkov ring, and a presumably different distribution of scattered background photons that reach the detector plane. This will inform the choice of a photocathode material, which should be optimized with respect to sensitivity to the signal and background photon wavelength distributions.

In the case of (x, y) strip readout, there is ambiguity about which of the multiple (x, y) combinations correspond to true photon coordinates. However, if location and momentum information (from other detectors) is available for tracks pointing at the Cherenkov module, ambiguities may be resolved. The simulations, including tracking by other detectors, will have to show if ring reconstruction using strip readout can be done in the environment of EIC events. If not, readout has to be done with pads or pixels, which would lead to much larger channel counts.

Specifically the tasks include:

- Model the optical elements: aerogel, lens, readout.

- Model the strip or pixel readout, and embed a detector in the EIC event environment, including tracking detectors. Determine maximal pixel/strip size, maximum module size (for modular concept), efficiency etc.
- Develop reconstruction software.

3.2. Characterization of LAPPDs

A few small (6×6 cm^2) LAPPD samples together with their front-end electronics will be provided by the ANL group.

The test will at least consist of the following items:

- Single photon detection efficiency at different wavelengths, particularly between UV and green,
- Background noise level,
- Gain as a function of input pulse rate,
- Time and position resolution,
- Radiation hardness,
- Sensitivity to magnetic field,
- Lifetime

Most of the performance tests will take place at Jefferson Lab in one of the two existing Hall-D testing spaces. Each room has a large dark box available for optics setups. Both spaces have been used previously for characterization of silicon photomultipliers (SiPMs) and PMTs used for Hall-D [21]. LEDs with different emission wavelengths will be procured to measure the photon detection efficiency (PDE). Existing equipment from Hall-D and the Detector Group, such as a high repetition rate picoseconds light pulser, optics, oscilloscopes, DAQ system with TDCs and ADCs, high/low voltage power supplies will be used to complete these tests.

For the PDE measurement test, the LED will be driven by a pulse generator. A narrow bandwidth filter will be used to select a specific wavelength and a set of neutral density filters allows one to precisely control the intensity of illumination. The absolute light intensity will be measured by a calibrated photodiode. The picosecond light pulser that Hall-D purchased from Hamamatsu is an ultrashort pulsed light source. It has less than 100 ps pulse width and the repetition rate can go up to 10 MHz. It provides an ideal light source to measure LAPPD's rate capability and timing resolution. The light can also be focused for position resolution measurement.

Background noise levels have been measured in 33 mm-diameter development MCPs by the LAPPD collaboration (see Figure 20) and have been shown to be quite low. This measurement needs to be repeated in a complete LAPPD assembly where noise from the photocathode could significantly increase the background rate. A preliminary measurement of gain versus rate has been measured for an older 10 μm pore MCP with an MgO SEE layer and is shown in Figure 21. Again this is a measurement that needs to be repeated and confirmed in a complete detector package.

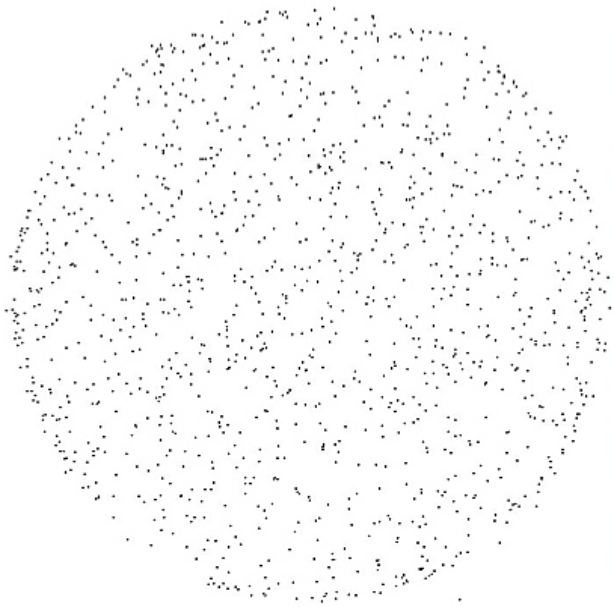

Figure 20 3000-second background collected on a 33 mm diameter ALD-MCP with 20 μm pores and 1.2mm thickness. The measured background is 0.84 counts/cm^2/s at 7×10^{-6} gain and is comparable to cosmic ray induced background.

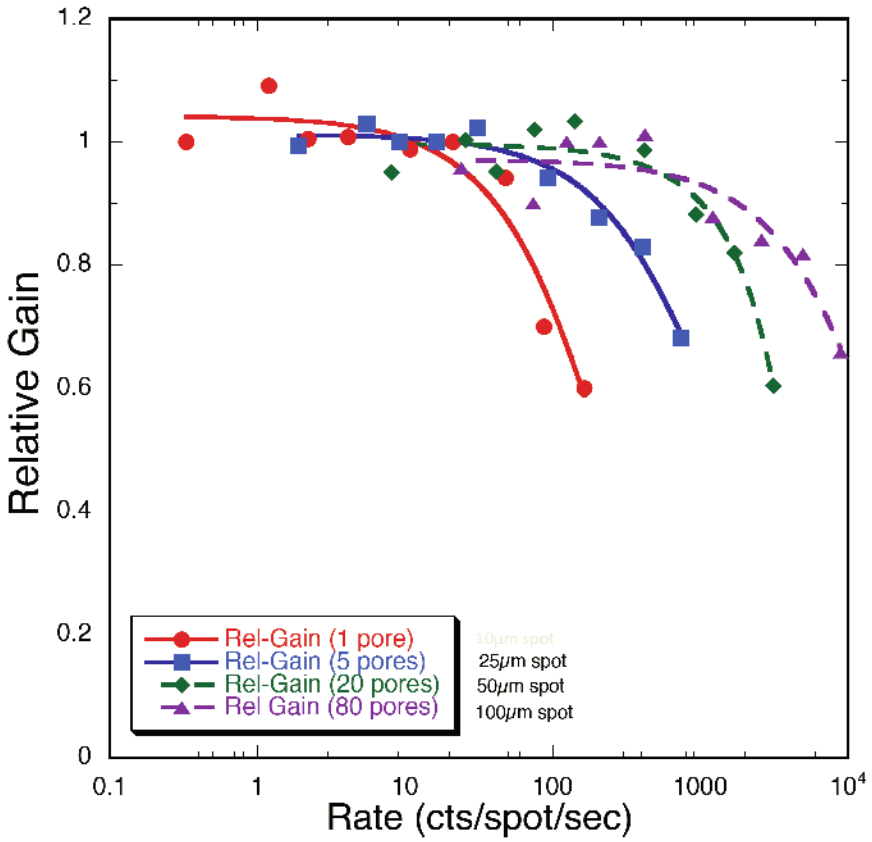

Figure 21 A preliminary measurement of gain as a function of rate for an older 10 μm pre MCP with an MgO SEE layer by O. Siegmund.

The radiation hardness test will be coordinated with the Jefferson Lab Radiation Control Group and both gamma and neutron irradiation sources will be used. A similar study has been performed on SiPMs [22][23]. Proton and neutron irradiation facilities are also available at Los Alamos. The effect of radiation damage on the photodetection efficiency, timing resolution, and gain as well as the noise level will be evaluated. In addition, Jefferson Lab has a spare-5 Tesla magnet dedicated for testing of magnetic field resistance of various detectors.

3.3. Improvement of LAPPD

Some characteristics of LAPPDs may need to be tuned in order to better fit the needs of its application in the EIC as well as other nuclear experiments. We identified a few items that may need more work besides the good timing/position resolution and cost that the LAPPD collaboration is already pursuing:

- High rate capability,
- Tolerance to strong magnetic field,
- Thinner glass window,
- Readout ambiguity with high rate/alternative charge collection option

For example, regarding the rate limitation, one may think of modifying the chemical composition of the ALD process to improve the discharging speed of the accumulated ions. This will help increase the rate tolerance, possibly at the expense of degraded timing resolution. In terms of window thickness, as many new types of strong glass have become available on the market, mainly driven by the needs of mobile phone industry, we can start to test different samples to see how well they can work as the current LAPPD window (2.75 mm thickness).

The readout ambiguity may become an issue for Cherenkov rings with very small radius, as many photons will hit a small area simultaneously. One possible way is to narrow the strip width to reduce the multiplicity in a single strip. Because the characteristic impedance of the strip line is a function of both strip width and glass thickness, such modification would need to be incorporated into an overall package redesign. If the hits are expected to be relatively far apart, a deconvolution algorithm may be implemented in the readout FPGA to further reduce signal overlaps. If needed, we will consider using 2-dimensional pixelated readout options.

These developments and improvements will be mainly carried out at Argonne National Laboratory taking advantage of the existing development facilities for the on-going LAPPD R&D project.

3.4. Study of GEM-Based Readout

While GEMs coated with CsI have been used to detect UV photons in previous experiments, the use of a GEM photocathode coating that is sensitive in the wavelength range appropriate for aerogel radiators (~ 300 – 500 nm) has not yet been realized on a

large scale. The first phase of photosensitive GEM development will focus on optimizing photocathode deposition parameters and operating gases to give the highest possible effective quantum efficiency (QE).

Triple-GEM detector kits, with an x-y strip readout plane and associated electronics, will be purchased from CERN. A suitable work area for testing and handling the GEM detectors will be set up on a laminar flow table at LANL. A small vacuum chamber for bialkali photocathode deposition onto the GEM surface will be assembled. Using an LED light source and a PMT of known QE as a reference, the QE of the photocathode will be measured in situ after deposition. The deposition rate and photocathode thickness will be varied to optimize the QE.

After the QE is established in vacuum, the chamber can be backfilled with a gas of choice to quantify the effect of the gas on the effective QE of the photocathode. In such a manner, along with bench measurements of GEM gain in the gas, a suitable operating gas can be chosen. In parallel with these laboratory measurements, a suitable readout pattern will be developed in simulation, which can maximize ring resolution while minimizing channel count. This readout pattern will then be tested on the bench.

3.5. Characterization and Selection of Aerogel Radiator

We will characterize different aerogel samples to choose the best option for the EIC RICH. The work will be conducted at Jefferson Lab by personnel from both INFN and Jefferson Lab. The proponents have developed skills for the optical characterization of the aerogel radiator for the CLAS12 RICH detector [7]. Some of the study will be carried at LANL as well.

The test will consist of the following items:

- Measurements of transmittance, absorption length and scattering length for different aerogel tiles,
- Measurements of refractive index and chromatic dispersion using the prims method,
- Refractive index mapping with gradient method,
- High precision mapping of the tiles thickness.

To perform measurements of transmittance, absorption length and scattering length a spectrophotometer will be used, while to measure the refractive index and the chromatic dispersion a monochromator coupled to a Xe-UV lamp and monochromatic lasers will fulfill our scope.

4. Expertise and Responsibilities

4.1. Jefferson Lab Hall-D/Detector Group

Jefferson Lab Hall-D and the Detector Group have a lot of experience in high energy particle detectors. Recently, the two groups together characterized various types of photomultiplier tubes and Silicon photomultipliers for the new GlueX spectrometer of Hall-D including their basic photodetection properties, radiation hardness and tolerance to magnetic field. The team was previously awarded of an EIC R&D proposal to study the improved radiation tolerant Silicon photomultipliers [23], and the same gamma and neutron irradiation facilities at Jefferson Lab will be used for this project. Jefferson Lab personnel have also been heavily involved in the design, construction and commissioning of several Cherenkov detectors used at Jefferson Lab, such as aerogel Cherenkov counters, light gas Cherenkov counters and a proximity focusing Freon RICH detector for Hall-A and the future aerogel RICH detector for the Hall-B CLAS12.

In this project, Jefferson Lab will mainly be responsible for the detector simulation, characterization of LAPPDs and conceptual design. The labor funding will be used to support a Jefferson Lab postdoc researcher to perform these tasks as well as characterization of aerogel radiators under the supervision of INFN.

4.2. Los Alamos National Lab Subatomic Physics Group

The LANL group has expertise with aerogel, in particular establishing the feasibility of using aerogel in imaging Cherenkov detectors [4][5]. LANL personnel developed, built and operated the PHENIX hadron-blind detector (HBD), a Cherenkov counter with photo-sensitive GEM readout and have experience in designing and building a micro-pattern readout and the associated custom data acquisition chain [24]. In addition, the team has also participated in designing and simulating a complete EIC detector.

LANL has neutron and proton irradiation facilities where radiation hardness of detector components can be studied. The team has recently conducted such studies. These facilities are available to collaborators.

In this project, LANL will be responsible for GEM photocathode manufacture and testing, optimizing RICH readout design, and will simulate and optimize the proposed RICH detector in a realistic EIC environment. The labor funding will be used to support a LANL postdoc researcher for the project.

4.3. Argonne National Lab High Energy Group

The ANL group is one of the leading groups of the DOE funded LAPPD project. The group has expertise in photocathode, micro-channel plate and fast readout electronics. The group has available facilities for large area photocathode coating, photocathode

characterization, atomic layer deposition, vacuum chamber for small LAPPD assembling and testing facility for LAPPD with a pulsed sub-picosecond laser.

ANL will fabricate LAPPD samples for the project. The team will also carry out the R&D of LAPPD towards the requirement of the EIC RICH readout. The labor funding will be mainly used to support an ANL postdoc researcher for the LAPPD fabrication and development.

4.4. INFN

INFN has extensive experience in RICH detectors and silica aerogels. Particularly, it is the leading group of developing the aerogel RICH detector for Jefferson Lab's CLAS12 spectrometer.

In this project, INFN will be responsible for characterization and selection of various aerogel samples for the EIC RICH detector.

5. Budgets

The budget needed to complete the proposed project is listed in Table 2.

Table 2 Budget breakdown for Phase I of the project

Item	Cost		
	Year 1	**Year 2**	**Year 3**
Jefferson Lab			
M&S – LAPPD testing	$10,000	$10,000	$10,000
Equipment – LAPPD testing	$20,000	$0	$0
Labor – Postdoc (0.7 FTE)	$70,000	$70,000	$70,000
Travel	$10,000	$10,000	$10,000
Subtotal	**$110,000**	**$90,000**	**$90,000**
Los Alamos National Lab			
GEM detector kits (5 ×$3200)	$16,000	$0	$0
CERN RD51 SRS Readout System	$3,000	$0	$0
Components for deposition chamber	$30,000	$20,000	$20,000
Labor – Post doc (0.4 – 0.5 FTE)	$60,000	$80,000	$80,000
M&S and Travel	$20,000	$20,000	$20,000
Subtotal	**$129,000**	**$120,000**	**$120,000**
Argonne National Lab			
M&S – LAPPD fabrication	$15,000	$15,000	$15,000
Labor – LAPPD fabrication and R&D	$50,000	$50,000	$50,000
Travel	$5,000	$5,000	$5,000
Subtotal	**$70,000**	**$70,000**	**$70,000**
INFN			
M&S – Aerogel Testing	$10,000	$10,000	$10,000
Equipment – Aerogel Testing	$30,000	$0	$0
Travel	$10,000	$10,000	$10,000
Subtotal	**$50,000**	**$20,000**	**$20,000**
Grand Total	**$359,000**	**$300,000**	**$300,000**

6. Further Work

With the completion of this proposed project, we expect to continue the project in a second phase to develop and fabricate a proof-of-principle prototype. With the chosen detector technology including radiators and readout, the collaboration will join the effort on prototyping such a detector.

Depending on the conceptual design provided by this project, the approach of future prototyping will vary. Using the GEM-based readout as an example, once a choice of gas has been made, and if the final effective quantum efficiency is sufficiently high to proceed with this technology, the production of sealed GEM chambers for beam tests will begin. Since bialkali photocathodes are notoriously reactive with air, the vacuum deposition chamber will be modified such that the GEM chambers can be sealed and removed from vacuum without exposure to atmosphere. Once sealed and removed from the deposition chamber, gas will be continually flowed through the GEM chamber to limit any contamination that may leak through. The GEM chambers can then be integrated with the aerogel radiator into a functional prototype, which can then be used in beam tests. The radiation damage effects on the photocathode can be carried out at LANL by exposing the chambers to proton and neutron beams available at.

By the end of the second phase, we will conduct necessary beam tests to demonstrate that the detector's performance will satisfy the EIC's needs on particle identification. As Jefferson Lab will have 12 GeV electron beams available by then, these tests will preferably take place at JLab and can be parasitic to other JLab experiments.

7. Summary

An R&D program is proposed to investigate the technology used for a Ring Imaging Cherenkov (RICH) detector for the hadron identification in the forward region of the future Electron-Ion Collider (EIC). Both the dual-radiator RICH option and a modular RICH concept will be investigated and the associated special optics design will be carried out. In particular, a newly developed Large-Area Picoseconds Photo-Detector (LAPPD) using renovated Micro-Channel Plate (MCP) technology will be carefully evaluated as the readout of the RICH detector. If feasible, the excellent timing resolution provided by this new readout will greatly improve the PID capability of the RICH detector. In parallel, a GEM-based readout option will be investigated as well. At the end, the project will be able to select the best detector technology and provide a conceptual design of the RICH detector for the EIC.

Bibliography

[1] *Electron Ion Collider: The Next QCD Frontier*, A. Accardi *et al.*, arXiv nucl-ex/1212.1701 (2012)

[2] ePHENIX Letter of Intent, PHENIX Collaboration, http://www.phenix.bnl.gov/plans.html

[3] *Use of silica aerogels in Cherenkov counters*, Y. N. Kharzheev, *Phys. of Part. and Nucl.*, 39, 1 (2008) 107

[4] *Use of aerogel for imaging Cherenkov counters*, D.E. Fields *et al.*, Nucl. Instr. and Meth. **A349** (1994) 431

[5] *A spot imaging Cherenkov counter*, H. Hecke, Nucl. Instr. and Meth. **A343** (1994) 311

[6] *Budker Institute of Novosibirsk and Boreskov Catalysis Institute of Novosibirsk, Novosibirsk, Russia*

[7] *The CLAS12 large area RICH detector, M. Contalbrigo*, E. Cisbani, P. Rossi, Nucl. Instr. and Meth. **A639** (2011) 302

[8] Matsushita-Panasonic Electric Works, Ltd., 1048 Kadoma, Osaka, Japan

[9] Aspen Aerogels, Inc., Northborough, MA, USA

[10] *Aerogel RICH for forward PID at Belle II*, R. Pestotnik *et al.*, Nucl. Instr. and Meth. **A732** (2013) 371

[11] *SUVT product details*, A&C Plastics Inc., http://acplasticsinc.com/techsheets/SUVT_ProductDetails.pdf

[12] *EIC Proposal RD6: Letter of Intent for Detector R&D towards an EIC detector*, K. Dehmelt *et al*.

[13] *The Development of Large-Area Fast Photo-detectors*, The LAPPD Collaboration, Proposal to the Department of Energy's Office of High Energy Physics (2009)

[14] *Development of sub-nanosecond, high gain structures of time-of-flight ring imaging in large area detectors*, the LAPPD collaboration, Nucl. Instr. and Meth. **A639** (2011) 148

[15] *Atomic layer deposited borosilicate glass microchannel plates for large area event counting detectors*, O.W. Siegmund *et al.*, Nucl. Instr. and Meth. **A695** (2012) 168

[16] *RF strip-line anodes for Psec large-area MCP-based photodetectors*, H. Grabas *et al.*, Nucl. Instr. and Meth. **A711** (2013) 124

[17] *A 15 GSa/s, 1.5 GHz Bandwidth Waveform Digitizing ASIC*, E. Oberia *et al.*, Nucl. Instr. and Meth. **A735** (2014) 452

[18] *A test-facility for large-area microchannel plate detector assemblies using a pulsed sub-picosecond laser*, B. Adams *et al.*, Rev. of Sci. Instr. **84** (2013) 061301

[19] *Design, construction, operation and performance of a Hadron Blind Detector for the PHENIX experiment*, W. Anderson *et al.*, Nucl. Instr. and Meth. **A646** (2011) 35

[20] *Progress in gaseous photomultipliers for the visible spectral range*, Breskin *et al.*, Nucl. Instr. and Meth. **A623** (2010) 318

[21] *Silicon photomultiplier characterization for the GlueX barrel calorimeter*, F. Barbosa *et al.*, Nucl. Instr. and Meth. **A695** (2012) 100
[22] *Radiation Hardness Tests of SiPMs for the JLab Hall D Barrel Calorimeter*, Y. Qiang *et al.*, Nucl. Instr. and Meth. **A698** (2013) 234
[23] *Proposal to Test Improved Radiation Tolerant Silicon Photomultipliers*, C. Zorn *et al.*, proposal to EIC R&D (2011)
[24] *The PHENIX Forward Silicon Vertex Detector*, C. Aidala *et al.*, arXiv:1311.3594